JOURNAL OF MATERIALS SCIENCE 27 (1992) 279–284

Rheological properties of Y–Si–Al–O–N glasses – elastic moduli, viscosity and creep

T. ROUXEL, M. HUGER, J. L. BESSON
Laboratoire des Matériaux Céramiques, LA CNRS 320, 87065 Limoges Cédex, France

Three oxynitride glasses from the Y–Si–Al–O–N system and differing in their N/O ratio were studied in the 800–1000 °C temperature range. Their viscosities were measured using a three-point bending test through the glass transition domain. For a given temperature, 4.8 wt% N_2 enhances the viscosity by three orders of magnitude in comparison with the corresponding oxide glass. Nitrogen also improves creep resistance. The activation enthalpy for creep, above T_g, is of the same order as those measured for silicon nitride ceramic (~ 900 kJ mol^{-1}). The elastic moduli were determined by ultrasonic techniques, from room temperature up to 1200 °C, which allowed calculation of the free activation enthalpy for viscous flow. Owing to the sharp decrease of shear modulus in the glass transition domain, the free activation enthalpy (~ 500 kJ mol^{-1}) greatly differs from the activation enthalpy usually measured in creep studies.

1. Introduction

Since it became evident that the high-temperature behaviour of silicon nitride-based ceramics was controlled by the characteristics of the grain-boundary glassy phases, interest in oxynitride glasses has been growing very rapidly [1, 2]. Extensive property measurements show that, compared with oxide glasses, oxynitride glasses, and especially those in the Y–Si–Al–O–N system, are much more resistant, in terms of hardness, elastic moduli and corrosion [3]. Therefore, such glasses are potential candidates for many structural applications. Although oxynitride glasses have been widely studied during the last 20 years, very few reports have been devoted to their mechanical properties at high temperature [4, 5], which are of major importance when one attempts to define the application field for such materials, or to gain a better understanding of the creep behaviour of silicon nitride-based ceramics. The present paper deals with elastic moduli, viscosity and creep resistance of Y–Si–Al–O–N glasses. The thermodynamics of the non-elastic deformation mechanisms that appear near the glass transition temperature domain was investigated with the aid of the thermally activated process analysis usually applied to crystal plasticity. This analysis has been motivated by the numerous papers reporting apparent activation energy for creep of Si_3N_4-based ceramics, but failing to identify clearly the operational quantities.

2. Materials

Three glass compositions were selected: V_1 is an oxide glass, V_2 and V_3 are oxynitride glasses with increasing amounts of nitrogen. The oxide glass was obtained by mixing appropriate quantities of silica, alumina and yttria powders. Nitrogen was incorporated by adding silicon nitride. The starting powders were wet-mixed in alcohol using a high-speed homogenizer. After the alcohol had been evaporated, a further period of dry-mixing was carried out to ensure homogeneity. The mixed powders were melted at 1700 °C for 1 h under a purified nitrogen atmosphere in graphite crucibles lined with boron nitride to prevent wetting, and quenched. Glasses were then annealed for 2 h at a temperature 50 °C below the glass transition temperature, to remove internal stresses.

The glass compositions are given in Table I. V_3 contains about one atom of nitrogen for five atoms of oxygen, which is close to the limit of solubility of nitrogen in such glasses. The nitrogen content has been verified experimentally using oxidation tests and the Kjeldhal method. Although no crystalline phase was detected by X-ray diffraction, all nitrogen glasses contain roughly spherical particles of about 0.5 μm diameter, that are disseminated in the matrix and are mainly constituted by free silicon [6].

The glass transition temperatures were determined by dilatometry. Tests were performed on rods (12 mm long, 2 mm diameter) in air at a heating rate of 5 °C min^{-1}.

3. Theory

3.1. General assumptions for activated flow

Below the glass transition temperature, glasses creep under constant stress (Fig. 1). This deformation recovers partially with ageing after unloading but a permanent strain still persists after a very long time. The whole deformation corresponds to the superposition of inelastic deformation and plastic flow.

0022–2461/92 $03.00 + .12 © 1992 Chapman & Hall

TABLE I Composition of the three grades

Grade		Composition					N_{exp}	Density ($g\,cm^{-3}$)	T_g (°C)
		Y	Si	Al	O	N			
V_1	wt %	38.3	18.1	6.7	36.9	0.0		3.88	863
	eq %	28	56	16	100	0			
V_2	wt %	39.4	18.6	6.8	31.4	3.8	3.7	4.00	911
	eq %	28	56	16	83	17			
V_3	wt %	39.9	18.8	6.9	28.8	5.6	4.8	4.12	926
	eq %	28	56	16	75	25			

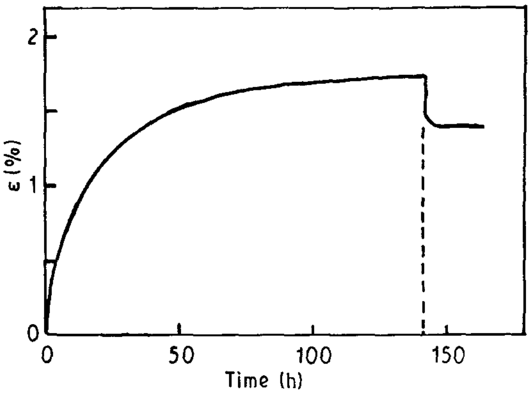

Figure 1 Creep and relaxation of glass V_2 under 30 MPa at 870 °C.

Argon [7] reviewed the inelastic deformation in amorphous solids and Escaig and co-workers [8, 9] developed a thermodynamic and kinetic analysis of non-elastic deformation in polymeric glasses by extending the thermodynamics and kinetics of activated plasticity established for crystals [10, 11]. Using this background we will attempt to outline a description of the deformation mechanisms in inorganic glasses.

In oxide glasses, strong covalent directional bonds maintain a near-neighbour coordination of chemically bonded species such as silicon–oxygen tetrahedra, giving rise to a distorted network broken from place to place at sites of network modifiers. The structure is characterized by a small amount of free volume. At temperatures below T_g, and in at least partially stabilized glasses, we expect that the free volume distribution will change only very slowly with time.

Without intending to propose a specific mechanism, we may consider that deformation arises from local rearrangements of flow units, that might be groups of Si–O tetrahedra in some kind of energy cage, formed by their nearest neighbours.

Of course, the glass structure is not a true equilibrium structure because of the slow decrease of its excess free energy. However, the characteristic relaxation time of this low ageing is relatively large ($\tau = 4$ h) and the cage structure of the glass can be considered as being in a quasi-equilibrium state for any response that does not require a time much larger than τ, which is the case for the thermal activation of plasticity [8]. To sum up, we consider that the deformation results from the rearrangements of flow units taking place in a quasi-fixed structure having a quasi-fixed free volume distribution. These transformations can be thermally assisted under applied stresses and their kinetics can be treated by the standard procedure of the transition state theory.

3.2. Thermodynamic definition of the activation parameters

We aim here to give proper definitions of the activation parameters and to show how these can be derived from data that are directly available from experiments. The minimum free enthalpy, ΔG_a, that has to be supplied for activation of flow units under a given applied stress, σ, corresponds to the deficiency in free enthalpy between the stable and the unstable equilibrium positions of the system $\Delta G_a = \Delta G_o - \Delta W_a$. The energy required for inelastic deformation is, therefore, the sum of a thermally originated term, ΔG_a, and a reversible work term, ΔW_a, done at the distant boundaries of the system. In the case of amorphous solids, Escaig and Lefebvre [8] have proposed the following expression

$$\Delta G_a = \Delta G_o - \sigma \Delta e_o V_c, \qquad (1)$$

where ΔG_o (σ, T) is the energy barrier height controlling the deformation process, Δe_o is the local shear strain appearing with the aid of thermal fluctuations, and V_c is the critical volume for nuclei to induce a plastic flow.

In the classical deformation temperature range, ΔG_a is described by the Maxwell–Boltzmann distribution and results in a macroscopic creep rate following an Arrhenius expression

$$\dot{\varepsilon} = A\sigma^n \exp[-\Delta G_a(\sigma, T)/(kT)] \qquad (2)$$

where $\dot{\varepsilon}$ is the strain rate, A a constant for a given material, σ the applied stress, n the stress exponent, ΔG_a the free enthalpy change during activation under the stress σ, and k is Boltzmann's constant.

Differentiation of the logarithmic form of this equation with respect to the temperature gives

$$[\partial \ln \dot{\varepsilon}/\partial T]_\sigma = [1/(kT^2)]\Delta G_a - [1/(kT)](\partial \Delta G_a/\partial T)_\sigma \qquad (3)$$

and

$$kT^2[\partial \ln \dot{\varepsilon}/\partial T]_\sigma = \Delta G_a - T(\partial \Delta G_a/\partial T)_\sigma \qquad (4)$$

According to the definition of the free enthalpy function, for an isothermal transformation

$$\Delta H_a = \Delta G_a + T\Delta S_a \qquad (5)$$

Comparison between the two latter expressions shows that the operational parameter which can be derived from a creep test by means of temperature jumps is the activation enthalpy

$$\Delta H_a = kT^2[\partial \ln \dot{\varepsilon}/\partial T]_\sigma \qquad (6)$$

It follows from Equation 5 that the free enthalpy is only obtainable if an evaluation of the main activation entropy contribution is made. In oxynitride glasses, where strong strain-localized effects should be nonexistent due to their highly directional bonds, we expect the activation entropy to be merely originating from the temperature dependence of the elastic moduli, which is rapid in the glass transition domain. This entropic term is assumed to be with a good approximation proportional to the shear modulus, μ, as it is in most cases for crystals.

It has been demonstrated by Gibbs [12] and by Schoek [10] that ΔG_a, which is the relevant activation energy, is thus given by

$$\Delta G_a = (\Delta H_a + x\sigma V_a)/(1 - x) \qquad (7)$$

with $x = (T/\mu)(\mathrm{d}\mu/\mathrm{d}T)$ where V_a is the activation volume, defined in agreement with the second law of thermodynamics by

$$\mathrm{d}(\Delta G_a) = -\Delta S_a \mathrm{d}T - V_a \mathrm{d}\sigma \qquad (8)$$

and

$$V_a = -[\partial \Delta G_a/\partial\sigma]_{T,\mathrm{struct.}} \qquad (9)$$

The activation volume can be directly expressed from Equation 2

$$V_a = kT[\partial \ln \dot{\varepsilon}/\partial\sigma]_{T,\mathrm{struct.}} - nkT/\sigma \qquad (10)$$

It is noticeable in this expression that the experimental quantity, directly available by means of a differential creep test at constant temperature for a given state of the material (i.e. at quasi constant time and strain conditions) is

$$V_{\mathrm{exp}} = kT[\partial \ln \dot{\varepsilon}/\partial\sigma]_{T,\mathrm{struct.}} \qquad (11)$$

Evans and Rawlings [11] suggested an estimation method for V_{exp} based on the measurement of strain rates both immediately before and after a jump of stress, the glass being first in a stationary flow state. In this way the glass does not have enough time to change during measurement.

4. Experimental procedure

4.1. Creep and viscosity

Creep tests were performed in air between 750 and 1000 °C in three-point bending with a span of 20 mm on bars with the following dimensions: 25 × 4 (width) × 3 (height) mm^3. The tensile stress on the outer fibre, σ, ranged from 5–90 MPa.

The expression for the viscosity, η, is based on the strong analogy existing between the stress/strain relations in an elastic solid and those governing a viscous fluid [13]

$$\eta = \sigma/[2(1 + \nu)\dot{\varepsilon}] \qquad (12a)$$

Generally Poisson's ratio, ν, is considered to be 0.5 for a viscous fluid and Equation 12a becomes

$$\eta = \sigma/3\dot{\varepsilon} \qquad (12b)$$

Hagy [14] has shown that beam-bending viscosity data agree well with fibre elongation measurements. The apparatus has been calibrated using a commercial silica glass (Corning "Vision"), the viscosity of which had been previously accurately determined by means of various techniques including fibre elongation and bending tests.

As a consequence of Equation 12a, the activation energy, ΔG_a, determined from the creep test is also the relevant activation energy for viscosity.

4.2. Elastic constants

To calculate ΔG_a from the measured free enthalpy, ΔH_a, the shear modulus and its temperature dependence have to be determined. Elastic moduli were measured using ultrasonic techniques.

At room temperature, the "Pulse Echo Overlap" technique [15] allows the measurement of the compressional, V_L, and shear, V_S, ultrasonic wave velocities with a better than 10^{-3} accuracy. The elastic moduli, E and μ, and hence ν are derived from the relations

$$E = \rho[3V_L^2 - 4V_S^2]/[(V_L/V_S)^2 - 1] \qquad (13)$$

$$\mu = \rho V_S^2 \qquad (14)$$

where ρ is the density.

High-temperature ultrasonic measurements require the thermal insulation of the transducer. The principle of the method is to use magnetostrictive transducers (remendur coils) which can generate ultrasonic pulses in long thin waveguides [16].

In the "long beam" mode approximation, Young's modulus is directly related to the compressional wave velocity (Equation 15) whereas the shear modulus is related to the torsional wave velocity, V_T, by Equation 16 [17]

$$E = \rho V_L^2 \qquad (15)$$

$$\mu = \rho V_T^2 \qquad (16)$$

Measurements were done in Ar–7% H$_2$ gas at a heating rate of 1 °C min^{-1} from room temperature to 1200 °C. The glass pieces available for the grades under study were too small to enable the preparation of samples long enough to be suitable for the direct determination of the shear modulus. Thus, only Young's modulus evolution was established.

However, both Young's and shear moduli were determined for another grade of oxynitride glass (Nd–Mg–SiON, 24–12–64–88–17 eq %) from room temperature to 100 °C above T_g. Comparison of the results showed that the temperature coefficients were identical for E and μ (Fig. 2) and that Poisson's ratio

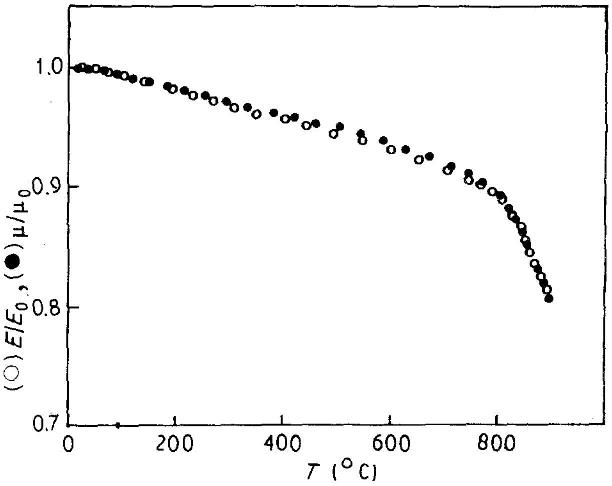

Figure 2 Evolution of E/E_0 and μ/μ_0 for an Nd–Mg–SiON glass from room temperature to 900 °C.

remained constant ($\nu = 0.29$) over the entire temperature range. So, we assumed that the same was true for glasses V_1, V_2 and V_3 under similar conditions. Taking $\nu = 0.5$ instead of $\nu = 0.29$ (that is using Equation 12b instead of Equation 12a) induces an undervaluation of the viscosity by 8%, which is within the overall precision and accuracy (= 10%) estimated by Hagy [14].

5. Results and discussion

5.1. Creep and viscosity

Typical creep curves for the three grades are plotted in Fig. 3. It was verified that no oxidation occurs for temperatures lower than 1050 °C. It is evinced by this figure that the presence of nitrogen leads to a significant decrease in creep strain. The transient creep is reduced and a quasi stationary stage is reached much more quickly.

The creep rate dependence on stress during stationary creep was measured from incremental stress steps at constant temperature (900 °C) for glass V_2. The stress exponent, $n = (\partial \ln \dot{\varepsilon}/\partial \ln \sigma)_T$, was found to be equal to 1.01, which suggests a linear viscoelastic behaviour.

Apparent viscosity curves are given in Fig. 4. The measured viscosities are in good agreement with those obtained above 950 °C for glass V_2 by Hampshire *et al.* [4], with the fibre elongation technique. Glass transition domains, empirically associated with viscosities ranging between 10^{12} and $10^{12.5}$ Pas, are close to the temperatures previously measured on similar materials using dilatometry and differential thermal analysis [6]. The higher the nitrogen content of the glass, the higher is the glass transition domain. Replacing bivalent oxygen atoms by trivalent nitrogen ones increases the interconnection degree in the glass network and results in a great improvement in rigidity and refractoriness. For a given viscosity, the temperature shift is about 80 °C between the oxide glass V_1 and the oxynitride glass V_3, and at a given temperature, the viscosity increases by three orders of magnitude.

It must be underlined that, due to the unstable nature of glass, measurements of physical properties in the glass transition domain are very delicate. The lower the temperature, below T_g, the more slowly does the glass become stable. This means that viscosities measured far below T_g, are likely to be underestimated. This could explain the curvature observed on the curves at the lowest temperatures.

5.2. Elastic constants

The room-temperature values of the elastic constants for the different grades are reported in Table II and illustrated by Fig. 5. Poisson's ratio is close to 0.3 in every case.

The $E(T)$ curves are shown in Fig. 6. When $T < T_g$, Young's moduli diminish slowly and linearly. However, as T approaches T_g, they decrease rapidly as a consequence of the softening of the glasses. Crystallization, which is indicated by an increase in the modulus, starts only above 900 °C for glass V_1 and above 1000 °C for glasses V_2 and V_3.

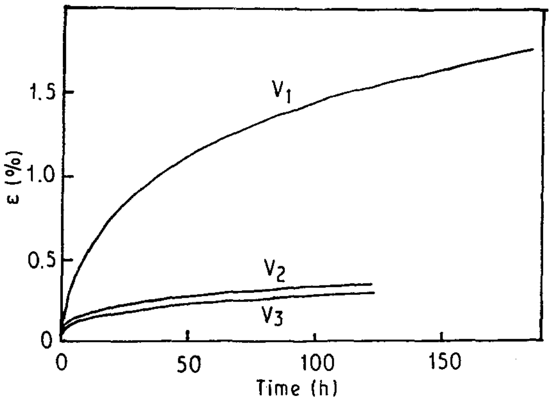

Figure 3 Three-point bending creep tests in air (90 MPa, 850 °C) for glasses V_1, V_2, V_3.

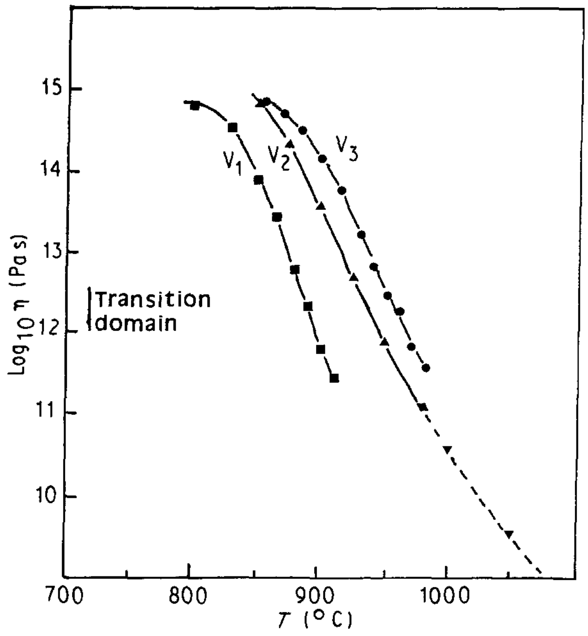

Figure 4 Dependence of the viscosity–temperature curve on nitrogen content: V_1 0 wt%, V_2 3.7 wt%, V_3 4.8 wt%, ▲ from [4].

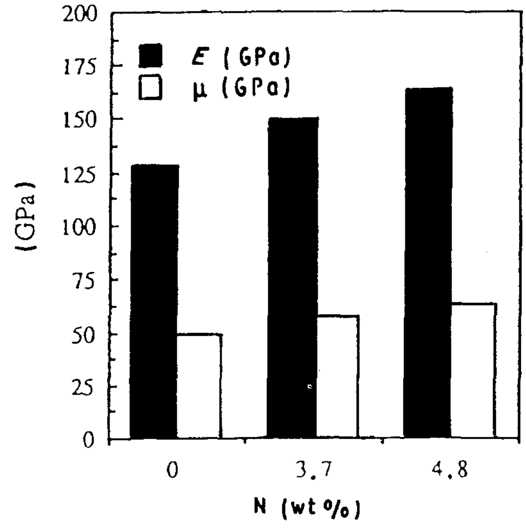

Figure 5 Elastic moduli, E and μ, at room temperature as a function of nitrogen content.

TABLE II Elastic moduli at room temperature

Grade	Young's modulus, E (GPa)	Shear modulus, μ (GPa)	Poisson's ratio	$\mathrm{d}E/\mathrm{d}T$, $T \ll T_g$ (GPa °C^{-1})
V_1	128	50	0.28	-13.9×10^{-3}
V_2	150	58	0.29	-16.3×10^{-3}
V_3	165	64	0.29	-17.9×10^{-3}

TABLE III Activation volumes for glass V_2

	850 °C	900 °C
$V_{exp}(10^{-29}\,m^3)$	73	757
$V_a(10^{-29}\,m^3)$	56 $(0.83\,nm)^3$	659 $(1.87\,nm)^3$

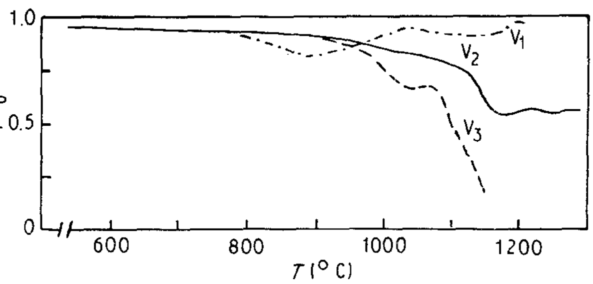

Figure 6 Relative Young's modulus versus temperature.

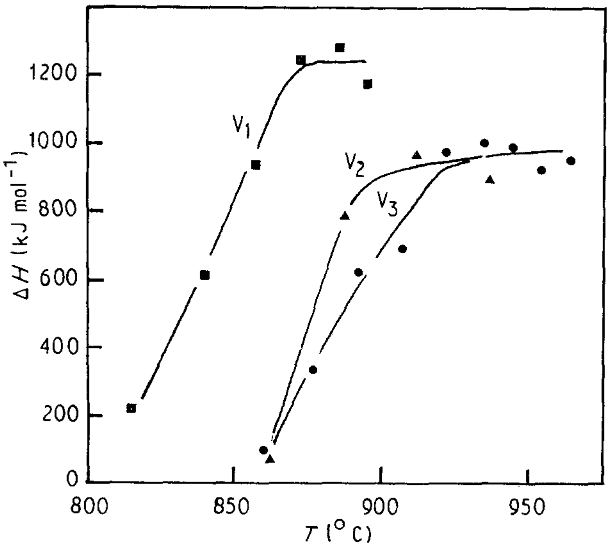

Figure 7 Activation enthalpy for creep, ΔH_a, versus temperature.

5.3. Activation parameters

Activation volumes calculated for glass V_2 from Equations 10 and 11 at 850 and 900 °C are reported in Table III. The results give an idea of the size of the flow units causing the plastic deformation. Volumes obtained at 850 and 900 °C correspond to two and six Si–(O, N)$_4$ tetrahedra, respectively.

The activation enthalpy, ΔH_a, was derived from Equation 6 from a creep test at constant stress (σ = 40 MPa). When replacing V_a by its numerical values in Equation 7 it was found that the second term of the numerator was obviously negligible and the expression for the activation free enthalpy reduces to

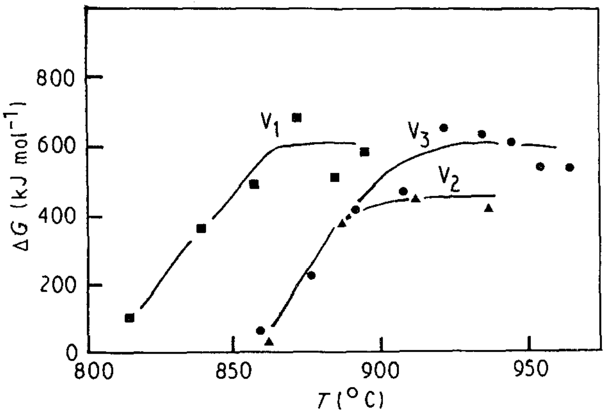

Figure 8 Activation free enthalpy for creep, ΔG_a, versus temperature.

$$\Delta G_a = \Delta H_a / \{1 - (T/\mu)(\mathrm{d}\mu/\mathrm{d}T)\} \quad (17)$$

ΔG_a was calculated assuming that ν remains constant and $(1/E)(\mathrm{d}E/\mathrm{d}T) = (1/\mu)(\mathrm{d}\mu/\mathrm{d}T)$ in the temperature range under consideration, as discussed in Section 4.2. ΔH_a and ΔG_a are plotted in Figs 7 and 8.

When $T \ll T_g$ the second term of the denominator $(T/\mu)(\mathrm{d}\mu/\mathrm{d}T)$ is very small and $\Delta G_a \neq \Delta H_a$. However, at temperatures near T_g, the relevant activation energy, ΔG_a, could no longer be assimilated to the apparent energy, ΔH_a.

5.4. Discussion

A tentative explanation can be proposed by analogy with the mechanical behaviour of polymeric glasses where, at low temperatures, only local rearrangements take place, whereas in the vicinity of the glass transition temperature, co-operative movements of long segments of chains (involving up to ten monomers) can occur [8].

The curves in Fig. 7, can be divided in two parts, separated by the glass transition domain. At low temperatures, the activation free enthalpy is low and the activation volume very small. The covalent bonds between atoms are strong as shown by the high values of the elastic moduli. This suggests that stresses can only be accommodated by very local rearrangements (such as rotation of individual Si–(O, N)$_4$ tetrahedra in the neighbourhood of a modifying cation) overcoming low-energy barriers. As the temperature rises, the atomic bonds weaken, and correlated motions of tetrahedra can be activated in increasing volumes. At T_g and above, the free activation enthalpy reaches a plateau, which suggests that most of the different flow units are then efficiently activated by thermal fluctuations.

6. Conclusions

1. Oxynitride glass refractoriness strongly depends

on the nitrogen content: the higher the nitrogen content, the higher is the glass transition domain. For instance, at a given temperature, viscosity is improved by three orders of magnitude between a Y–Si–Al–O glass and a 4.8 wt% N_2-containing Y–Si–Al–O–N glass. However, the temperature gain for a given viscosity is only 80 °C. Furthermore, nitrogen greatly reduces the total strain and the viscoelastic effect in glasses during creep tests.

2. The apparent activation energy for creep of silicon nitride-based ceramics reported by most of the authors is an activation enthalpy and roughly coincides with the activation enthalpy measured above 925 °C (beginning of the plateau) on an oxynitride glass containing 4.8 wt% N_2. The latter is 900 kJ mol^{-1}, whereas the apparent energy reported for creep of silicon nitride-based ceramics ranges between 780 [18] and 850 kJ mol^{-1} [19]. This result confirms the major importance of the glassy phase on the creep behaviour of these ceramic materials.

3. The use of thermodynamics of thermally activated deformation allows calculation of the free activation enthalpy for non-elastic deformation of a glass from the available operational quantities. However, knowledge of the change of the elastic constants as a function of temperature is required. Furthermore the analysis provides an evaluation of other quantities such as the activation volume and entropy. A framework for explanation is proposed for the mechanical mechanisms, but further investigations are required, especially on the structure of these glasses, to clarify this point.

Acknowledgements

The authors are grateful to Professor S. Hampshire, University of Limerick, Ireland, for supplying the nitrogen glasses, and Professor C. Gault, E.N.S.C.I. Limoges, France, for allowing the use of the ultrasonic equipment.

References

1. G. LENG-WARD and M. H. LEWIS, "Glasses and glass ceramics", edited by M. H. Lewis (Chapman and Hall, London, 1988) p. 106.
2. R. E. LOEHMAN, *J. Non-Cryst. Solids* **56** (1983) 123.
3. S. HAMPSHIRE, R. A. L. DREW and K. H. JACK, *Phys. Chem. Glasses* **26** (1985) 182.
4. *Idem, Commun. Amer. Ceram. Soc.* **3** (1984) C 46.
5. T. ROUXEL, J. L. BESSON, C. GAULT and P. GOURSAT, in "1st EcerS, Euro Ceramics", Vol. 3 – "Engineering Ceramics", Maastricht, June 1989, edited by G. de With, R. A. Terpstra and R. Metselaar (Elsevier Applied Science, London, 1990) p. 351.
6. T. ROUXEL, Ph.D thesis, Limoges (1990).
7. A. S. ARGON, in "Glass: Science and Technology", Vol. 5, edited by D. R. Uhlmann and N. J. Kreidl (Academic Press, London, 1980) p. 79.
8. B. ESCAIG and J. M. LEFEBVRE, *Rev. Phys. Appl.* **13** (1978) 285.
9. J. P. CAVROT, J. HAUSSY, J. M. LEFEBVRE and B. ESCAIG, *Mater. Sci. Engng* **36** (1978) 95.
10. G. SCHOECK, *Phys. Status Solidi* **8** (1965) 499.
11. A. G. EVANS and R. D. RAWLINGS, *ibid.* **34** (1969) 9.
12. G. B. GIBBS, *Phil. Mag.* **16** (1967) 97.
13. F. T. TROUTON, *Proc. Roy. Soc. Lond.* **77** (1906) 426.
14. H. E. HAGY, *J. Amer. Ceram. Soc.* **46** (1963) 93.
15. H. J. Mc SKIMIN, *J. Acoust. Soc. Amer.* **33** (1961) 12.
16. C. GAULT, in "Materials Research Society Symposium Proceedings on Non-Destructive Monitoring of Materials Properties", Vol. 142 edited by J. Holbrook and J. Bussiere (Materials Research Society, Pittsburg, 1989) p. 263.
17. J. E. MAY Jr, in "Physical Acoustics", Vol. I, part A, edited by W. P. Mason (Academic Press, New York, 1964) p. 428.
18. A. BOUARROUDJ, P. GOURSAT and J. L. BESSON, *J. Mater. Sci.* **20** (1985) 1150.
19. R. M. ARONS and J. K. TIENS, *ibid.* **15** (1980) 2046.

Received 7 January
and accepted 13 May 1991